Gallic Acid Is an Antagonist of Semen Amyloid Fibrils That Enhance HIV-1 Infection*[S]

Josephine G. LoRicco[‡1], **Changmingzi Sherry Xu**[‡], **Jason Neidleman**[§], **Magnus Bergkvist**[¶], **Warner C. Greene**[§], **Nadia R. Roan**[§‖2], and **George I. Makhatadze**[‡3]

From the ‡*Center for Biotechnology and Interdisciplinary Studies and Department of Biological Sciences, Rensselaer Polytechnic Institute, Troy, New York 12180, the* §*Gladstone Institute of Virology and Immunology, San Francisco, California 94158, the* ¶*Colleges of Nanoscale Science and Engineering, SUNY Polytechnic Institute, Albany, New York 12203, and the* ‖*Department of Urology, University of California, San Francisco, California 94158*

Recent *in vitro* **studies have demonstrated that amyloid fibrils found in semen from healthy and HIV-infected men, as well as semen itself, can markedly enhance HIV infection rates. Semen fibrils are made up of multiple naturally occurring peptide fragments derived from semen. The best characterized of these fibrils are SEVI (semen-derived enhancer of viral infection), made up of residues 248–286 of prostatic acidic phosphatase, and the SEM1 fibrils, made up of residues 86–107 of semenogelin 1. A small molecule screen for antagonists of semen fibrils identified four compounds that lowered semen-mediated enhancement of HIV-1 infectivity. One of the four, gallic acid, was previously reported to antagonize other amyloids and to exert anti-inflammatory effects. To better understand the mechanism by which gallic acid modifies the properties of semen amyloids, we performed biophysical measurements (atomic force microscopy, electron microscopy, confocal microscopy, thioflavin T and Congo Red fluorescence assays, zeta potential measurements) and quantitative assays on the effects of gallic acid on semen-mediated enhancement of HIV infection and inflammation. Our results demonstrate that gallic acid binds to both SEVI and SEM1 fibrils and modifies their surface electrostatics to render them less cationic. In addition, gallic acid decreased semen-mediated enhancement of HIV infection but did not decrease the inflammatory response induced by semen. Together, these observations identify gallic acid as a non-polyanionic compound that inhibits semen-mediated enhancement of HIV infection and suggest the potential utility of incorporating gallic acid into a multicomponent microbicide targeting both the HIV virus and host components that promote viral infection.**

Amyloid fibrils are ordered protein aggregates associated with a large number of human diseases, many of which are neurodegenerative in nature, such as Alzheimer disease and Parkinson disease (1–3). They are characterized by their cross-β structure, with β sheets running perpendicular to the fibril axis, and by their ability to bind to certain fluorescent dyes, such as thioflavin T (ThT),[4] whose fluorescence intensity increases considerably upon binding to amyloid fibrils.

Amyloid fibrils are also found in semen from young, healthy men (4). Whether these fibrils serve a physiological function is not known, but they have been shown to markedly increase infection by a variety of sexually transmitted viruses, most notably HIV-1 (5–7). Under limiting dilution conditions, semen fibrils can increase HIV infection rates by up to 5 orders of magnitude (6). These fibrils are made up of naturally occurring peptide fragments in semen (6, 8–10). The best characterized semen fibril is made up of a 39-residue fragment from human prostatic acid phosphatase (PAPf39) and has been termed SEVI (semen-derived enhancer of viral infection) (6). More recently, a second set of semen fibrils was identified from prostate-specific antigen-generated fragments of semenogelin (referred to collectively as SEM1 fibrils when in fibrillar form), the predominant component of the semen coagulum (9, 10). Mechanistic studies have revealed that the cationic nature of both SEVI and SEM1 fibrils is important for their ability to enhance HIV infection. In particular, anionic polymers prevent binding of the fibrils to HIV and cellular targets and abrogate infection-enhancing activity (10, 11). Furthermore, substitution of the lysine and arginine residues of PAPf39 with alanines generated a peptide that could still form amyloid fibrils but lacked the ability to enhance HIV infection (11). These data suggest that semen fibrils promote infection by decreasing the electrostatic repulsion between HIV virions and their cellular targets. However, the fibrillar nature of SEVI and SEM1 fibrils is also important for activity because the cationic monomeric peptides that

Gallic Acid Is an Antagonist of Semen Amyloids

are the precursors of SEVI and SEM1 fibrils completely lack the ability to enhance HIV infection (6, 10, 12).

Because semen fibrils not only markedly enhance HIV infection but also decrease the potency of microbicides targeting the HIV virus (13), antagonizing their activity may improve the efficacy of topical HIV microbicides. Although anionic polymers, such as heparin, have been found to be effective at eliminating the enhancement of HIV infection by SEVI and SEM1 fibrils *in vitro* (10, 11), polyanionic microbicide candidates have proved largely ineffective and potentially even harmful in clinical trials, due to their propensity to increase rather than decrease transmission rates (14). This may have been caused by the ability of some polyanions, such as nonoxynol-9, to induce an inflammatory response that can promote HIV infection by recruiting target cells and up-regulating HIV gene transcription (15). As such, there have been efforts to identify non-polyanionic compounds that inhibit the activity of semen fibrils while avoiding eliciting an inflammatory response. A variety of non-polyanionic compounds have been identified that through binding semen fibrils antagonize their activity, and a subset of these compounds retain activity in seminal plasma (SP) (16 – 20). To date, however, a small molecule that inhibits semen fibril activity by completely disassembling preformed fibrils has not been pursued.

To this end, in this study, we conducted a small molecule screen for compounds that can disassemble preformed semen fibrils, using a fluorescence-based assay with ThT. We identified from this screen the compound gallic acid, a phenol found in grape seed extract. Gallic acid has been shown to inhibit formation of α-synuclein, insulin, and amyloid-β amyloid fibrils (21 – 25). It is structurally related to the polyphenol epigallocatechin-3-gallate, a natural component found in green tea that was previously demonstrated to prevent formation of SEVI fibrils from PAPf39 monomers and to even degrade preformed fibrils (18, 26, 27). Here, we characterize the effects of gallic acid on SEVI and SEM1 fibrils using the amyloid-binding dye ThT; by measuring zeta potentials; and by confocal, atomic force, and electron microscopies. We show that contrary to our original hypothesis, gallic acid does not disassemble preformed fibrils but rather binds the fibrils to quench ThT fluorescence and alter their surface charge.

Experimental Procedures

Peptide Purification—PAPf39 peptide NH$_2$-GIHKQKEKSR-LQGGVLVNEILNHMKRATQIPSYKKLIMY-COOH (6, 28, 29) was synthesized at the Penn State College of Medicine Macromolecular Core Facility. PAPf39 was dissolved in 0.05% TFA and purified on a C18 reverse-phase HPLC column (Discovery Bio Wide pore C18 10 μm, 25 cm × 10 mm; Supelco Sigma-Aldrich, Bellefonte, PA) using a methanol gradient in the presence of 0.05% TFA.

SEM1(86 – 107) peptide NH$_2$-DLNALHKTTKSQRHLGGS-QQLL-COOH (12) was purchased from Celtek Peptides at 98% purity (Franklin, TN). The peptide was dissolved in 0.05% TFA and purified on a C18 reverse-phase HPLC column (Discovery Bio Wide pore C18 10 μm, 25 cm × 10 mm; Supelco Sigma-Aldrich) using a gradient of acetonitrile with 0.065% TFA.

The mass of each peptide was confirmed using MALDI mass spectrometry. Samples for MALDI analysis were prepared by diluting the sample 5-fold with the matrix supernatant. The matrix was prepared by dissolving 10 mg of α-cyano-4-hydroxycinnamic acid (52.9 mM) in 1 ml of water, 50% acetonitrile, 0.01% TFA; vortexing; and centrifuging the solution at 14,000 rpm for 10 min to remove undissolved material. Measurements were performed on a Bruker Ultraflex III MALDI TOF/TOF (Bruker Biosciences, Billerica, MA) in the Rensselaer Polytechnic Institute Proteomics Core facility and processed using the Micromass TOF Spec 2E Mass Spectrometer software suite. For each peptide, the fractions containing the pure peptide were pooled and subjected to three cycles of lyophilization and resuspension in Milli-Q water to remove residual TFA.

Peptide Concentrations—Peptide concentrations were measured using a UV-visible spectrophotometer (U-2900 Hitachi, Tokyo, Japan). PAPf39 peptide was diluted in the desired buffer such that the absorbance at 280 nm was <1 unit. UV spectra were collected from 370 to 240 nm in 0.2-nm increments. Peptide concentrations were determined using a molar extinction coefficient of 2,980 M^{-1} cm^{-1} at 280 nm.

SEM1(86 – 107) does not contain any aromatic residues, so the concentration was determined using the absorbance at 205 nm. Concentration measurements were performed in 0.1 M potassium sulfate, 5 mM monopotassium phosphate adjusted to pH 7.0 with potassium hydroxide. SEM1(86 – 107) was diluted into the measurement buffer such that the absorbance at 205 nm was between 0.3 and 0.8 (1,000-fold dilution of ~12 mg/ml peptide). The concentration was determined using an extinction coefficient of 27 ml mg^{-1} cm^{-1} at 205 nm. All concentrations are expressed per monomer of PAPf39 or SEM1(86 – 107).

Fibril Preparation—SEM1 fibrils, which correspond to fibrillized SEM1(86 – 107) peptide, were prepared by dissolving lyophilized SEM1(86 – 107) peptide in 3.5 mM hydrochloric acid. The concentration was estimated from absorbance at 205 nm as described above and adjusted to 7.5 mg/ml. PAPf39 fibrils were prepared by dissolving dry PAPf39 peptide in 3.5 mM hydrochloric acid. The concentration was estimated from the absorbance at 280 nm as described above and adjusted to 6 mg/ml. These stock solutions of PAPf39 or SEM1(86 – 107) were diluted 3-fold in a dilution buffer (1 part peptide stock solution to 2 parts 18 mM PBS) to yield a final concentration of 2.5 mg/ml for SEM1(86 – 107) and 2 mg/ml for PAPf39. The samples were prepared on ice, and fibril formation was facilitated by agitating the samples at 37 °C for 24 h in a gyratory water bath shaker (model G76, New Brunswick Scientific, Edison, NJ) at 180 rpm (speed 6) or at 1,400 rpm with an Eppendorf Thermomixer. For fibrillation kinetics in the presence of gallic acid, samples were supplemented with 0.5 mM freshly prepared gallic acid in PBS. At desired time intervals, 10-μl samples were withdrawn and mixed with 40 μl of 150 mM Congo Red in PBS and 500 ml of PBS to give a final volume of 550 μl (final Congo Red concentration 10.9 μM). The changes in Congo Red fluorescence intensity at 610 nm (emission maximum) after excitation at 540 nm were recorded and averaged for 90-s intervals. 10 μM Congo Red in PBS without the peptides was used as a blank. Measurements for each time point were done in triplicate, and averaged values and S.D. values are reported.

Milli-Q water (Millipore, Billerica, MA) was used to prepare all buffers. 10-Fold concentrated PBS, pH 7.7, stock solution was composed of 1.37 M sodium chloride (NaCl), 27 mM potassium chloride (KCl), 101.4 mM sodium phosphate dibasic, 17.6 mM potassium phosphate monobasic, and 0.3076 M sodium azide (0.2%, w/v). This stock solution (120 mM) was then diluted 10-fold, and the pH adjusted to generate a working solution of 12 mM PBS, pH 7.7. The 18 mM PBS, pH 8.1, dilution buffer was prepared by diluting the 10× PBS stock (120 mM) with water and adjusting the pH with sodium hydroxide. It was prepared such that a 2:1 dilution of 18 mM PBS, pH 8.1, with 3.5 mM hydrochloric acid, pH 2.5, would yield PBS, pH 7.7, which has the same composition as the working solution of PBS described above.

ThT and Gallic Acid Measurements—ThT was purchased from Thermo Fisher Scientific. A ThT stock solution was made by dissolving the dry powder in 20 mM phosphate buffer, pH 7.7, at a concentration of 1 mM. 20 mM sodium phosphate buffer (PB), pH 7.7, was prepared through a 10-fold dilution of a 10× concentrated stock solution of 200 mM sodium phosphate, pH 7.7 (consisting of 78.85 mM sodium phosphate monobasic, 121.5 mM sodium phosphate dibasic, and 0.2% (w/v) sodium azide, pH 7.7).

Anhydrous gallic acid (3,4,5-trihydroxybenzoic acid) was purchased from Alfa Aesar (Ward Hill, MA). A 1 mM stock solution of gallic acid was freshly prepared before the ThT fluorescence measurements by dissolving gallic acid in 12 mM PBS. This solution was then diluted to the desired gallic acid concentration (between 25 and 500 μM).

ThT fluorescence assays were performed at 37 °C on a Fluoromax-4 spectrofluorometer (Horiba Jobin Yvon, Kyoto, Japan) in a 10-mm path length quartz cuvette. Samples were excited at 440 nm, and the emission was collected at 482 nm for 90 s and averaged. The fluorescence intensity was corrected for fluctuations in lamp intensity by dividing the fluorescence signal by the lamp intensity.

Fibrils were diluted to a concentration of 125 μg/ml in 400 μl by the appropriate gallic acid-containing solution just before the ThT fluorescence measurement. This solution was mixed and added to the cuvette. Next, the ThT stock solution was added such that the final ThT concentration was between 1 and 50 μM ThT in a final volume of 550 μl. The final concentration of the fibrils was 90.9 μg/ml. As a control, we demonstrated that gallic acid had no impact on ThT fluorescence in the absence of amyloid fibrils (data not shown).

Fibril Pelleting—Gallic acid was prepared at a final concentration of 0, 100, 500, or 1,000 μM in PBS. Preformed fibrils were then incubated with the different gallic acid concentrations for 2 h at room temperature and then centrifuged at 14,000 rpm for 30 min at 4 °C. As a positive control, concentrated hydrochloric acid was added to fibrils to lower the pH to 2.5, conditions that completely dissociate fibrils (28–30). The supernatant was then removed, and the pellet was resuspended in 100 μl of PBS, pH 7.7. The pellet was then incubated with 10 μM Congo Red, and fluorescence emission was recorded at 610 nm after excitation at 540 nm. The averaged value and the S.D. from triplicate experiments are reported.

Small Molecule Screen—A total of 137,872 compounds were tested for the ability to disassemble the HIV-enhancing SEM1 fibrils described previously (12). A final compound concentration of 20 μM in 0.1% DMSO was added to preformed amyloids. After a 2-h incubation, 5 μM ThT was added. Because ThT emits strong fluorescence at 482 nm only when bound to amyloid fibrils, we screened for compounds that decreased the ThT signal in the presence of the amyloids. We used ThT-treated amyloids in the presence of DMSO as negative controls and ThT in the absence of amyloids as positive controls. Assay wells with calculated inhibition exceeding the mean + (3 × S.D.) (68%) formed the initial hit list (320 compounds, 0.23% hit rate). These were further tested for the ability to inhibit SP-mediated enhancement of HIV infection in TZM-bl cells using established assays (5, 10). Four compounds reproducibly inhibited the ability of SP to enhance HIV infection without decreasing target cell viability. One of these, gallic acid was further investigated in this study. All screening was conducted at the University of California (San Francisco, CA) (UCSF) Small Molecule Discovery Center.

Infection Assay—Infectivity assays were performed using methods similar to those described previously (5, 10). 293T cells were transfected with CCR5-tropic 81A proviral DNA by Fugene (Promega, Madison, WI) and assayed for p24-Gag content by ELISA (PerkinElmer Life Sciences). The supernatant was diluted to 100 ng/ml p24-Gag and treated for 2 h with SP or amyloid at the indicated pretreatment concentrations, in the absence or presence of 500 μM gallic acid. Treated virions (20 μl) were then added to 10^4 TZM-bl cells (280 μl). To minimize toxic effects caused by prolonged exposure of SP to target cells, the medium was replaced after 2 h, and infection was assayed 3 days later by quantitating β-galactosidase activity (Gal-Screen kit from Life Technologies, Inc.). Background signals obtained from uninfected cells were subtracted from values obtained with infected cells. Infection assays were always accompanied by a cytotoxicity assay (CellTiter-Glo®) to monitor cellular viability.

Confocal Microscopy—Glass slides were purchased from VWR (25 × 75 mm, 1.0 mm thick). Coverslips were purchased from Fisher (Fisherfinest™ Premium Cover Glasses, size 22 × 22 mm, thickness No. 1). Glass slides and coverslips were soaked in 30% ethanol overnight to remove any dust before use.

Confocal images were acquired using a Zeiss LSM 510 META laser-scanning confocal microscope equipped with a diode laser (405 nm), argon lasers (458 nm, 488 nm), an HeNe laser (543 nm), and a ×100 (Zeiss α Plan-Fluar, oil immersion, 1.45 numerical aperture) objective. Pinhole was set to be close to 1 airy unit to reduce the signal/noise ratio. To image ThT fluorescence, the sample was excited with the 405-nm laser, and emission was collected using a 505–530-nm band pass filter. To image Congo Red-stained fibrils, samples were excited with the 458-nm argon laser, and emission was collected with a 505-nm long pass filter. Raw images were exported from an LSM image browser in 16-bit TIFF format with no compression.

Atomic Force Microscopy (AFM)—AFM images were acquired using AC tapping mode in air at room temperature and humidity on an MFP-3D atomic force microscope (Asylum Research, Santa Barbara, CA), using a silicon-coated cantilever
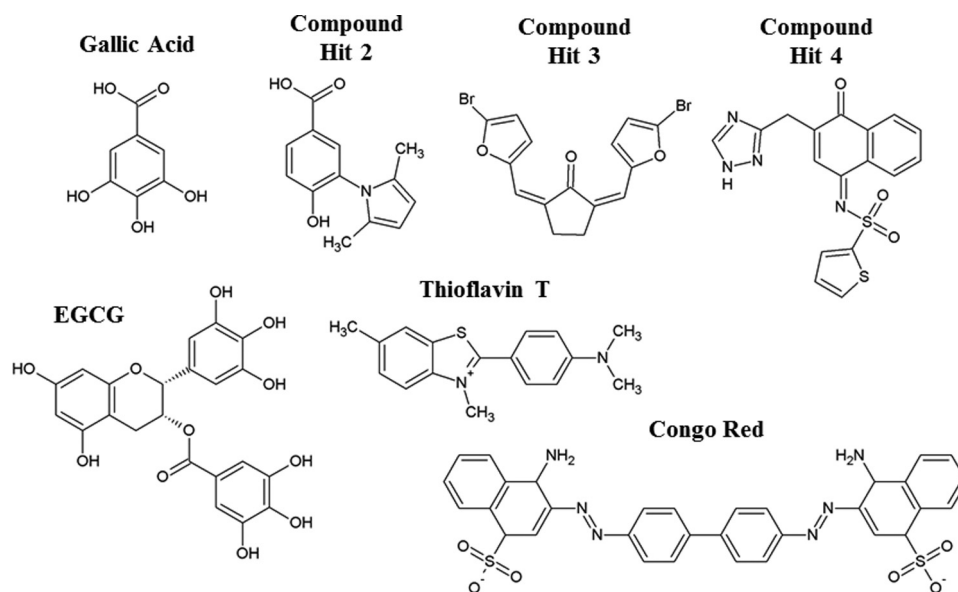
FIGURE 1. **Gallic acid and the three other primary hits that inhibited SP-mediated enhancement of HIV infection.** Shown are the chemical structures of each compound. The chemical structure of epigallocatechin-3-gallate (*EGCG*) is presented to highlight the structural similarities to gallic acid. In addition, chemical structures of the amyloid-binding compounds ThT and Congo Red are shown.

with a tip radius of 9 nm, resonant frequency of 70 kHz, and spring constant of 2 newtons/m (AC240TS, Olympus America Inc., Center Valley, PA). AFM images were analyzed in Igor Pro MFP3D software (Wavemetrics Inc., Portland, OR).

AFM plates were prepared by fixing a square of mica to a glass slide and spotting $10-20$ μl of sample onto freshly cleaved mica. Samples were incubated at room temperature for 20 min, followed by a gentle wash with 3 ml of Milli-Q water to remove buffer salts. The plates were allowed to air-dry before imaging.

Zeta Potential—Zeta potential measurements were taken on a Zetasizer Nano ZS (Malvern Instruments Ltd., Worcestershire, UK). The measurements were performed at 25 °C and analyzed using the Malvern Zetasizer software assuming Smoluchowski conditions.

Fibrils were preformed in PBS. Because the salt concentration in PBS was too high for reliable zeta potential measurements, fully formed fibrils in PBS, pH 7.7, were centrifuged at 14,000 rpm for 10 min. The supernatant was removed, and the pellet was resuspended in 1 ml of 20 mM PB to a final concentration of 0.2 mg/ml. Sodium phosphate buffer (20 mM), pH 7.4, was prepared as described above.

The gallic acid stock solution was prepared by dissolving gallic acid powder in 20 mM PB, pH 7.4. Gallic acid was added to the fibrils in PB such that the final concentration of gallic acid was 0, 0.1, 0.5, or 1.0 mM. The ascorbic acid stock solution was made by dissolving ascorbic acid powder in PB. All measurements were made with samples that contained 50 μM ascorbic acid to prevent oxidation of the gallic acid solution. Fibrils were incubated in the presence of gallic acid for 2 h before zeta potential measurements.

Effect of Gallic Acid on SP-induced Inflammation—De-identified endometrial biopsies were provided by the UCSF Endometrial Tissue Bank (institutional review board approval 14-15361). Stromal fibroblasts were isolated from the biopsies and then cultured as described previously (31). Cells were seeded in 24-well tissue culture plates and cultured until con-

fluence. At the initiation of the assay, cells were treated with 1% SP or the equivalent volume of PBS. Where indicated, wells were treated with the non-steroidal anti-inflammatory drug sulindac (500 μM) as a positive control or with an active concentration of gallic acid (10 μM). This concentration has been previously shown to almost completely block induction of IL-6, TNF-α, and other inflammatory cytokines by various stimuli (32, 33). After 6 h, culture supernatants were collected for IL-6 quantitation by ELISA (Life Technologies). All conditions were tested in experimental triplicates.

Results and Discussion

To identify compounds that can disassemble semen fibrils, we conducted a small molecule screen. For screening, we chose the previously described SEM1(86–107) fibrils (hereafter referred to as SEM1 fibrils) (12) because the peptide forming these fibrils is abundant (on average $\sim$100 μg/ml for SEM1 compared with $\sim$35 μg/ml for SEVI (6, 12)) and simpler to synthesize on a large scale due to its short length compared with the SEVI peptide. The entire chemical library of 137,872 compounds available for screening at the UCSF Small Molecule Discovery Center was tested for the ability to disassemble preformed SEM1 fibrils using a ThT assay. This assay takes advantage of the ability of ThT to emit strongly at 482 nm when bound to fibrils (1, 2, 29, 34, 35) and can be used to monitor semen fibril formation from monomeric peptide (4, 6, 28–30, 36). Compounds exhibiting inhibition exceeding the mean $+$ ($3 \times$ S.D.) (68%) formed the initial hit list. This list consisted of 320 compounds, corresponding to a 0.23% hit rate. These hits were cherry-picked and tested for the ability to inhibit SP-mediated enhancement of HIV infection in TZM-bl cells. Only four of the 320 hit compounds reproducibly inhibited SP-mediated enhancement of HIV infection (Fig. 1). Of these, three were previously uncharacterized, whereas the remaining one, gallic acid, is a natural component of grape seeds and has previously been reported to be an antagonist of several amyloid
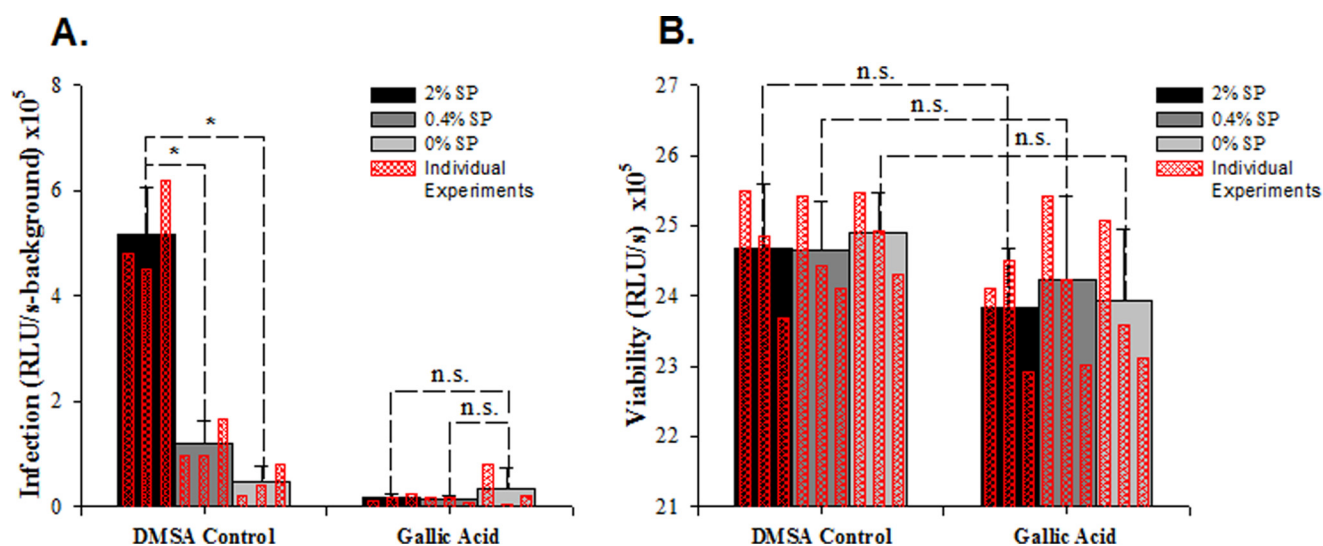
FIGURE 2. **Gallic acid inhibits SP-mediated enhancement of HIV infection (A) without compromising cellular viability (B).** Gallic acid (0.5 mM) or the equivalent amount of DMSO was incubated with the indicated concentration of SP for 2 h, added to the CCR5-tropic HIV-1 strain 81A, and diluted 15-fold upon the addition to TZM-bl cells. Infection levels were assessed 3 days later by quantitating β-galactosidase activity (with signal from uninfected cells subtracted). Viability was assessed by cellular ATP levels (by CellTiter-Glo®). Averaged values and S.D. values of triplicate experiments are shown as *solid bars*, whereas the results of individual measurements are shown as an *overlay* in *hatched red bars*. *, $p < 0.05$, Student's t test. *n.s.*, not significant.
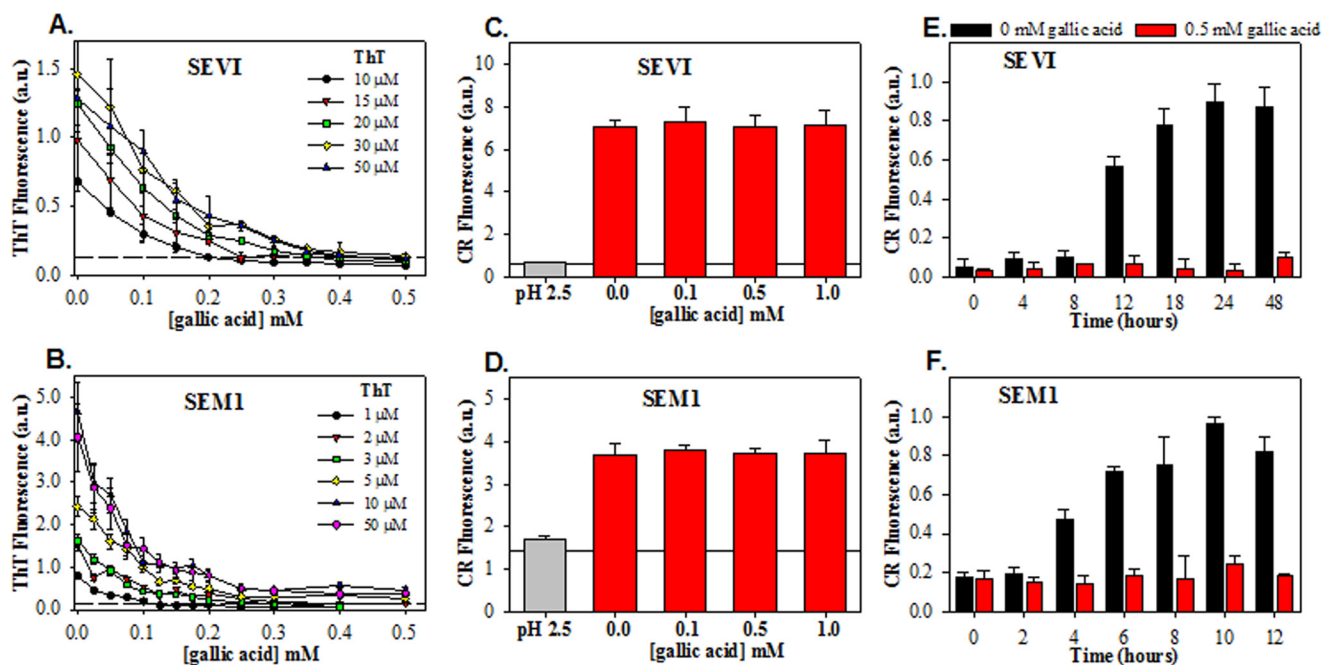

FIGURE 3. **Effects of gallic acid on biophysical properties of SEVI and SEM1 fibrils.** Shown is competition between gallic acid and ThT for binding to SEVI fibrils (*A*) and SEM1 fibrils (*B*). ThT fluorescence was measured in the presence of a fixed concentration of fibrils (90 μg/ml) with the indicated concentrations of ThT and gallic acid. *Horizontal dashed lines* in *A* and *B* indicate the intrinsic ThT fluorescence in the absence of fibrils. Solubility, as assessed by centrifugation of SEVI (*C*) and SEM1 (*D*) preformed fibrils in the absence and presence of 1 mM gallic acid, is independent of gallic acid. *Horizontal lines* in *C* and *D* show the intrinsic fluorescence of Congo Red in the absence of fibrils. Effect of gallic acid of fibrillation kinetics of PAPf39 (*E*) and SEM1(86–107) (*F*) shows that gallic acid is an effective inhibitor of both SEVI and SEM1 fibril formation. Averaged values and S.D. values (*error bars*) of triplicate experiments for each data point are shown. *a.u.*, arbitrary units.

fibrils (23–25). We confirmed in a separate set of assays that gallic acid inhibits SP-mediated enhancement of HIV infection in the absence of inducing cellular toxicity (Fig. 2). To better understand the mechanism by which gallic acid inhibits SP-mediated enhancement of HIV infection, we set out to characterize its molecular interactions with SEVI and SEM1 fibrils.

We first tested for a dose response in gallic acid-mediated inhibition of ThT fluorescence in the presence of semen fibrils.

Mature SEVI and SEM1 fibrils were generated in PBS, pH 7.7, added to different concentrations of gallic acid, and then immediately examined in a ThT assay. At ThT concentrations of 10–50 μM, the fluorescence signal at 482 nm mediated by SEVI decreased in response to increasing concentrations of gallic acid (Fig. 3A). When SEVI was treated with 500 μM gallic acid, the ThT signal was closer to the intrinsic fluorescence values of ThT than the fluorescence of ThT bound to amyloid fibrils.
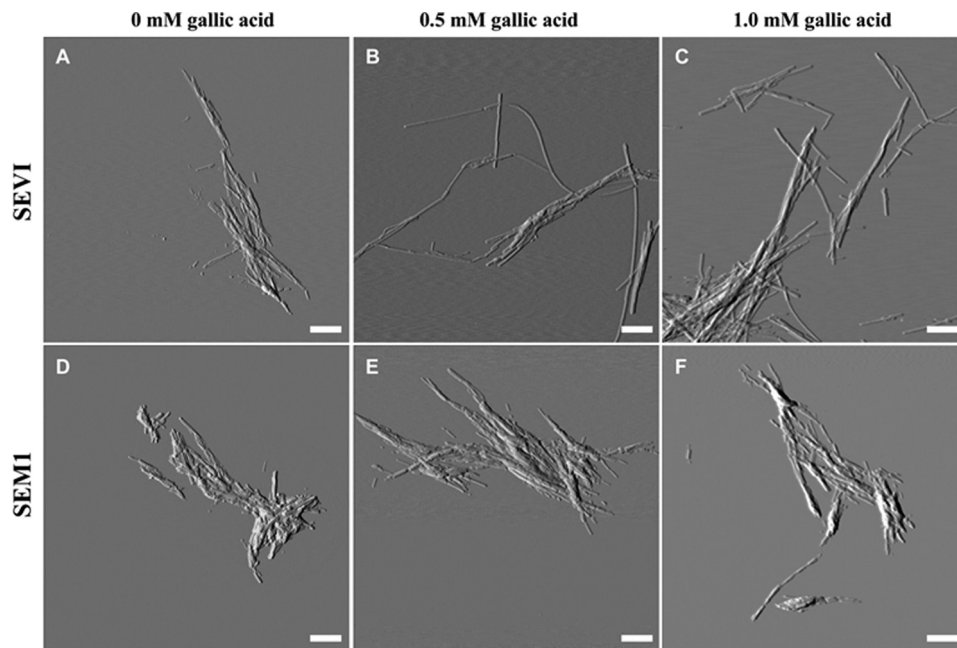
FIGURE 4. **Atomic force microscopy images of SEVI fibrils (*A–C*) and SEM1 fibrils (*D–F*) in the presence of 0 mM gallic acid (*A* and *D*), 0.5 mM gallic acid (*B* and *E*), and 1 mM gallic acid (*C* and *F*).** Preformed fibrils were incubated with gallic acid for 20 min on mica prior to imaging. *Scale bar*, 500 nm.

SEM1 fibril fluorescence in the presence of ThT was also diminished in a dose-dependent manner by gallic acid (Fig. 3*B*); however, the signal never reached intrinsic ThT fluorescence levels, as seen with SEVI.

Because a lower ThT signal is often equated with a smaller quantity of amyloid fibrils, the data suggest that gallic acid disassembles preformed SEVI and SEM1 fibrils. Moreover, because gallic acid decreased the ThT signal in the presence of SEVI down to nearly the intrinsic ThT fluorescence level, it was possible that complete SEVI fibril dissociation was occurring. To test whether this was indeed the case, we conducted AFM measurements to determine whether the fibrils were eliminated by gallic acid. Contrary to our prediction, the AFM measurements indicated that SEVI retained its fibrillar structure in the presence of gallic acid at concentrations exceeding those that eliminated ThT fluorescence (Fig. 4, *A–C*). SEM1 fibrils were similarly left intact in the presence of gallic acid (Fig. 4, *D–F*). The morphologies of the SEVI and SEM1 fibrils were both not altered by the addition of gallic acid (Fig. 5). Electron micrographs confirmed that gallic acid does not disassemble preformed semen fibrils (supplemental Fig. 1). These data suggest that although the ThT signal of semen fibrils decreased upon the addition of gallic acid, this was probably not due to dissociation of the fibrils.

Confocal microscopy was then employed to confirm that the decrease in ThT signal upon the addition of gallic acid was not due to the disassembly of SEVI or SEM1 fibrils. The final concentrations of SEVI and SEM1 fibrils used for confocal microscopy were the same as those used in the ThT assays. Amyloid fibrils were visualized through the bright field channel simultaneously with fluorescence measurements. In the absence of gallic acid, ThT bound to both SEVI and SEM1 fibrils, and areas of high ThT fluorescence matched up with bright field detection of amyloid aggregates (Fig. 6, *A*, *D*, *G*, and *J*). In the presence of
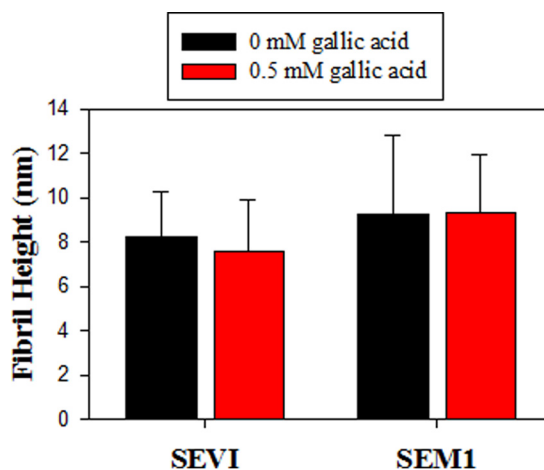

FIGURE 5. **Structural morphology of fibrils in the absence and presence of 0.5 mM gallic acid.** Fibril heights were measured from AFM images using Igor Pro MFP3D software. A *line* was drawn across individual fibrils, and a *two-dimensional trace* of the image surface was generated and used to determine fibril height. At least three images were analyzed for each condition (>150 measurements). The average fibril height is reported, and *error bars* represent S.D. values in fibril height.

1 mM gallic acid, SEVI fibrils were still readily visible by bright field but no longer visible on the ThT channel (Fig. 6, *B* and *E*). Gallic acid also decreased ThT fluorescence of SEM1 fibrils but to a lesser extent than that observed with SEVI (Fig. 6, *H* and *K*). These data are consistent with the notion that gallic acid decreases the ThT fluorescence values in the presence of SEVI down to intrinsic levels but suggest that this effect is due to replacement or quenching of the ThT molecules by gallic acid rather than by disassembly of the fibrils.

ThT fluorescence is known to be affected by a variety of compounds in the environment, particularly polyphenols (37). For this reason, we repeated the confocal microscopy experiments using Congo Red instead of ThT to image the fibrils. Congo Red
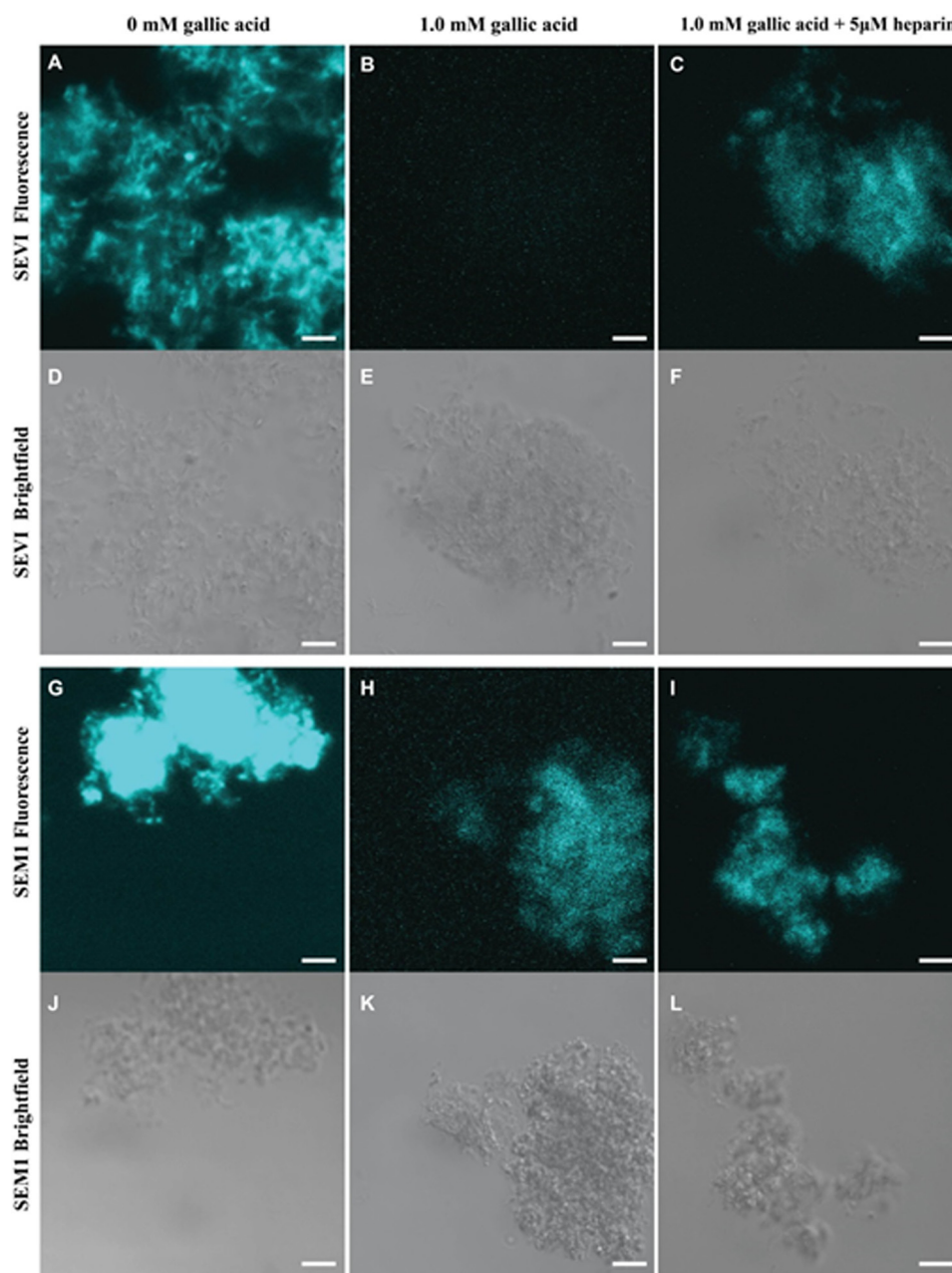
FIGURE 6. **Confocal microscopy images of amyloid fibrils visualized either by fluorescence microscopy (*A–C* and *G–I*) or by bright field microscopy (*D–F, J–L*) in the presence of 50 μM ThT.** SEVI (*A–F*) or SEM1 (*G–L*) fibrils were imaged at a concentration of ∼90 μg/ml. Fibrils were imaged in the presence of either 0 mM gallic acid, 1 mM gallic acid, or 1 mM gallic acid with 5 μM heparin. *Scale bar*, 5 μm.

is another amyloid-binding dye and, when bound to fibrils, exhibits green birefringence under polarized light in addition to increased fluorescence (1, 38, 39). Congo Red bound both SEVI and SEM1 fibrils, and importantly, this binding was not affected by gallic acid (Fig. 7). Therefore, imaging by AFM, electron microscopy, and confocal microscopies, together with Congo Red staining, all demonstrated that gallic acid does not disassemble SEVI or SEM1 fibrils. These data provide a cautionary lesson for screens designed to identify amyloid disassemblers through use of the ThT assay because this compound can exhibit changes in fluorescence in a manner independent of fibril disassembly.

To confirm that gallic acid was not affecting fibril solubility, we performed pelleting experiments. Fibrils were incubated with gallic acid and then pelleted by low-speed centrifugation. As shown in Fig. 3, *C* and *D*, gallic acid did not alter the amount of fibrils that were pelleted by centrifugation, demonstrating that gallic acid had no effect on the solubility of mature fibrils. Interestingly, however, the addition of gallic acid to monomeric peptides inhibited fibril formation (Fig. 3, *E* and *F*), consistent with prior reports of gallic acid as a fibrillation inhibitor (21–25).

The data suggest that the decrease in ThT fluorescence must be caused not by fibril dissociation but by some alternative mechanism(s). One possibility is that gallic acid directly competes with ThT for binding sites on the fibrils such that dissociation of ThT from fibrils causes the decrease in ThT fluorescence intensity. The second possibility is that gallic acid binds to the fibrils in such a way that it leads to quenching of ThT
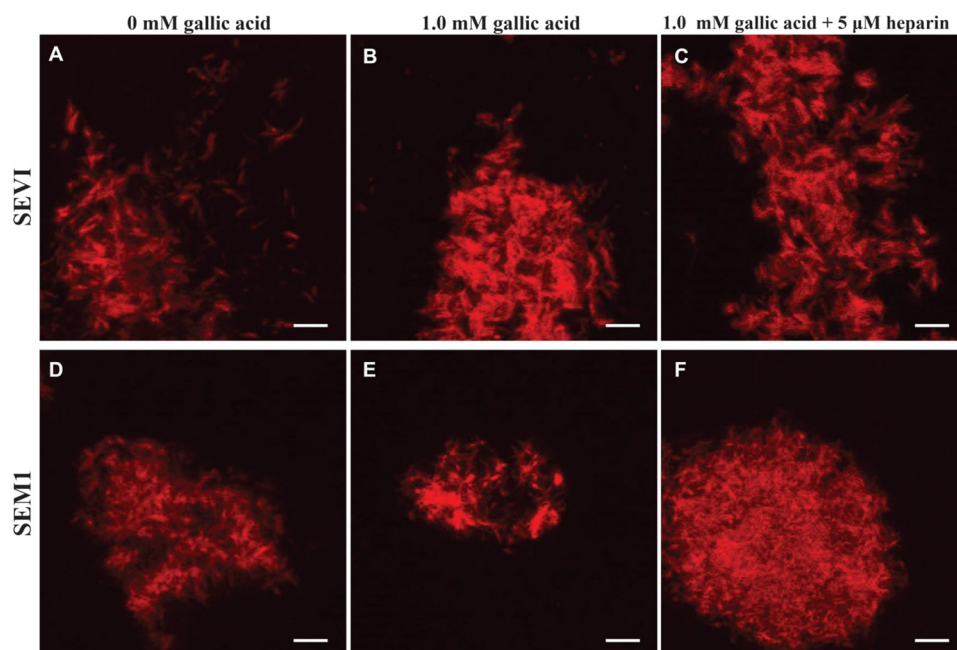
FIGURE 7. Confocal microscopy images of amyloid fibrils visualized in the presence of 50 μM Congo Red. SEVI (*A–C*) or SEM1 (*D–F*) fibrils were imaged at a concentration of ~90 μg/ml. Fibrils were imaged in the presence of 0 mM gallic acid, 1 mM gallic acid, or 1 mM gallic acid with 5 μM heparin. *Scale bar*, 5 μm.

fluorescence. Under both of these scenarios, as the concentration of gallic acid increases, ThT fluorescence would decrease, as a result of either displacement or quenching. The data in Fig. 3 had examined ThT fluorescence using ThT concentrations from 10 to 50 μM. When the curves for titrations performed with two different concentrations of ThT overlap, then signal saturation has been reached. For SEVI, the saturation point was reached at 30 μM ThT because further increasing the ThT concentration to 50 μM produced a curve that overlapped with the 30 μM curve (Fig. 3*A*). A saturation effect qualitatively similar to that observed with SEVI was also observed with the SEM1 fibrils; however, saturation occurred at the lower ThT concentration of 10 μM (Fig. 3*B*). Fitting the data in Fig. 3 to a binding model (40) that accounts for direct competition of ThT and gallic acid for fibril binding failed to generate a good fit. This suggests, by process of elimination, that gallic acid binding probably leads to the quenching of ThT fluorescence.

Having established that gallic acid binds instead of disassembles semen fibrils, we then proceeded to characterize the nature of this binding. PAPf39 and SEM1 are highly cationic peptides that contain a high proportion of basic residues (11, 12). Eight of the 39 residues of PAPf39 and 3 of the 22 residues of SEM1(86–107) are lysine or arginine residues (21 and 14%, respectively). The theoretical isoelectric point of PAPf39 is 10.2 (11), whereas that of SEM1(86–107) is 10.0 (12). Because ThT also has a positive charge, it could encounter electrostatic repulsion when in contact with the SEVI or SEM1 fibrils. To determine whether electrostatic interactions are important for the binding of gallic acid, heparin, a highly negatively charged glycosaminoglycan, was added to gallic acid-treated fibrils. When heparin was added to gallic acid-treated SEVI, it partially restored the detection of SEVI with ThT through confocal microscopy, suggesting that heparin and gallic acid compete for binding to the fibrils (Fig. 6*C*). Gallic acid-treated SEM1 fibrils

could also be readily detected by ThT staining when heparin was added (Fig. 6*I*). In contrast, binding of the gallic acid-treated fibrils to Congo Red, which has a negative charge, was unaffected by heparin (Fig. 7). These data suggest that electrostatics probably play a role in gallic acid binding to semen fibrils.

To further explore the role of electrostatics in the interaction of gallic acid with the fibrils, we measured zeta potential. Zeta potential is a measure of the electrokinetic potential at the slipping plane of a particle in solution. It is often used to determine the colloidal stability of a solution, which is dependent on the electrostatic repulsion between particles. Zeta potential is related to the effective surface charge of a particle in solution (41). Thus, changes in zeta potential upon treatment of SEVI and SEM1 fibrils with gallic acid reflect how gallic acid alters the surface properties of these fibrils. Zeta potential of the fibrils was measured in the presence of various concentrations of gallic acid. The zeta potential for both SEVI and SEM1 fibrils significantly decreased as the concentration of gallic acid was increased from 0 to 1 mM: from 8.2 $\pm$ 0.1 to 5.6 $\pm$ 0.4 mV for SEVI and from -9.1 ± 1.7 to -27.7 ± 2.5 mV for SEM1 fibrils (Fig. 8). These data suggest that gallic acid, which at neutral pH is negatively charged (pK_a = 4.4), binds the semen fibrils and in this manner decreases their zeta potential.

Overall, the biophysical data suggest that gallic acid inhibits semen-mediated enhancement of HIV infection not by disassembling preformed fibrils but rather by coating the surface of these fibrils and changing their electrostatic properties. Importantly, however, gallic acid is not a polyanion, a group of compounds that electrostatically coat the surface of semen fibrils but have failed in clinical trials because they tended to increase rather than decrease transmission risk. Polyanions tend to be pro-inflammatory (15), whereas gallic acid has anti-inflammatory properties (32, 33, 42). As such, gallic acid has the potential
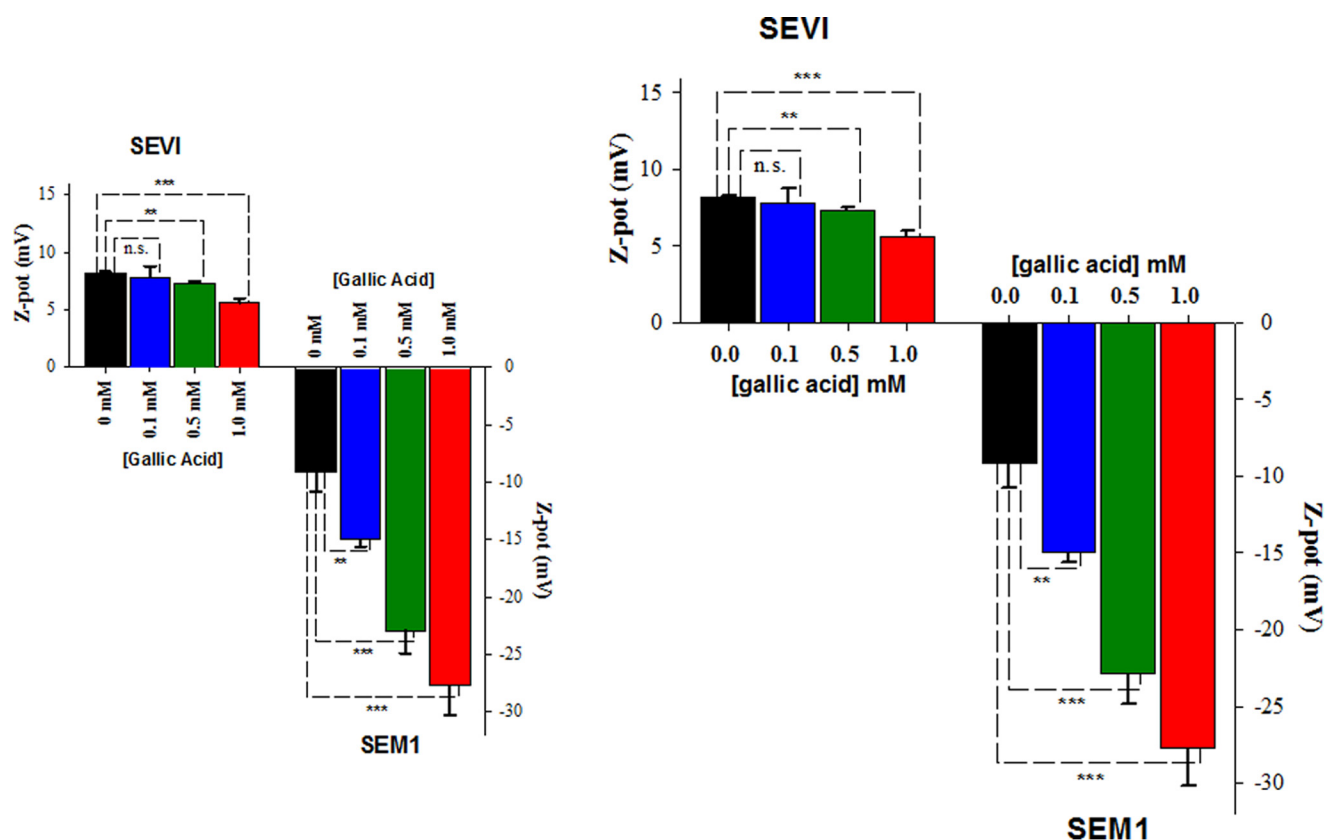
FIGURE 8. **Zeta potential of SEVI (*left*) and SEM1 (*right*) fibrils in the presence of increasing concentrations of gallic acid.** Fibrils were preformed in PBS at pH 7.7 and then resuspended in PB for zeta potential measurements. Averaged values and S.D. values (*error bars*) of triplicate experiments for each data point are shown. **, $p < 0.01$; ***, $p < 0.001$, Student's *t* test. *n.s.*, not significant.

to not only antagonize semen fibril activity but to additionally prevent an excessive inflammatory response, which could promote transmission by up-regulating HIV gene transcription and/or by recruiting cellular targets (43– 46). In the final part of the study, we further characterized the anti-inflammatory properties of gallic acid. SP induces a massive pro-inflammatory response in cells of both the lower and upper female reproductive tract (31, 47, 48). Because this type of inflammation presumably occurs during sexual transmission of HIV, we tested whether gallic acid can diminish SP-induced inflammation. Primary endometrial stromal fibroblasts were purified from endometrial biopsies and treated with SP. After 6 h, IL-6, a canonical pro-inflammatory cytokine, was significantly induced compared with mock-treated cells (Fig. 9). Gallic acid, used at a concentration previously reported to completely block inflammatory cytokine induction (including IL-6) in response to various stimuli (32, 33, 42), did not diminish this SP-mediated IL-6 induction, whereas the non-steroidal anti-inflammatory drug sulindac did (Fig. 9). These data suggest that the previously reported anti-inflammatory properties of gallic acid are not effective at preventing SP-induced inflammation in cells of the genital mucosa. As such, it is likely that other anti-inflammatories will need to be included to develop a mixture microbicide that both inhibits semen fibril activity and limits the HIV infection-promoting inflammatory response in the genital mucosa. Reassuringly, gallic acid does not induce inflammation, both in the absence and presence of SP (Fig. 9), in contrast to previous polyanionic microbicides, such as nonoxyl-9 (15).
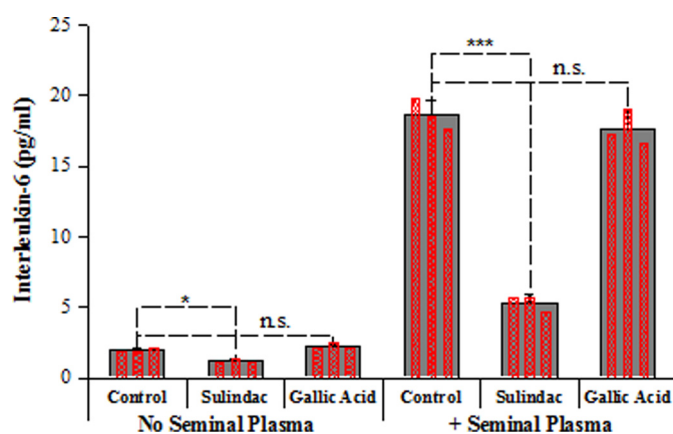

FIGURE 9. **Gallic acid does not prevent SP-mediated induction of IL-6 secretion.** Primary endometrial stromal fibroblasts were incubated in the absence or presence of 1% SP for 6 h in the presence of the non-steroidal anti-inflammatory drug sulindac or an active concentration of gallic acid, and then culture supernatants were collected for IL-6 quantitation by ELISA. Averaged values and S.D. values of triplicate experiments are shown as *solid bars*, whereas the results of individual measurements are shown as an overlay of *hatched red bars*. *, $p < 0.05$; ***, $p < 0.001$ in Student's *t* test. *n.s.*, not significant.

In conclusion, gallic acid, a previously described amyloid antagonist that we pulled out of a screen designed to identify semen fibril disassemblers, does not disassemble semen fibrils but rather binds directly to them. This conclusion is based on our finding that in the presence of gallic acid, intact fibrils are visible by AFM, electron microscopy, and confocal microscopy.

Gallic Acid Is an Antagonist of Semen Amyloids

This binding, which occurs for both SEVI and SEM1 fibrils, is sufficient to limit SP-mediated enhancement of HIV infection. This is probably mediated by a change in the surface charge of the fibrils. These data reinforce the importance of the cationic property of semen fibrils for their ability to enhance HIV infection (10, 11) and suggest that identifying compounds that completely disassemble semen fibrils may be challenging. Unlike polyanions, gallic acid is not pro-inflammatory, although it cannot limit the inflammatory response induced by SP. These data suggest that gallic acid, when combined with other anti-inflammatories, may be useful to incorporate into a multicomponent combination microbicide that targets both the HIV virus and host factors that promote HIV transmission.

References

1. Buxbaum, J. N., and Linke, R. P. (2012) A molecular history of the amyloidoses. *J. Mol. Biol.* **421,** 142–159
2. Chiti, F., and Dobson, C. M. (2006) Protein misfolding, functional amyloid, and human disease. *Annu. Rev. Biochem.* **75,** 333–366
3. Goldschmidt, L., Teng, P. K., Riek, R., and Eisenberg, D. (2010) Identifying the amylome, proteins capable of forming amyloid-like fibrils. *Proc. Natl. Acad. Sci. U.S.A.* **107,** 3487–3492
4. Usmani, S. M., Zirafi, O., Müller, J. A., Sandi-Monroy, N. L., Yadav, J. K., Meier, C., Weil, T., Roan, N. R., Greene, W. C., Walther, P., Nilsson, K. P., Hammarström, P., Wetzel, R., Pilcher, C. D., Gagsteiger, F., *et al.* (2014) Direct visualization of HIV-enhancing endogenous amyloid fibrils in human semen. *Nat. Commun.* **5,** 3508
5. Kim, K. A., Yolamanova, M., Zirafi, O., Roan, N. R., Staendker, L., Forssmann, W. G., Burgener, A., Dejucq-Rainsford, N., Hahn, B. H., Shaw, G. M., Greene, W. C., Kirchhoff, F., and Münch, J. (2010) Semen-mediated enhancement of HIV infection is donor-dependent and correlates with the levels of SEVI. *Retrovirology* **7,** 55
6. Münch, J., Rücker, E., Ständker, L., Adermann, K., Goffinet, C., Schindler, M., Wildum, S., Chinnadurai, R., Rajan, D., Specht, A., Giménez-Gallego, G., Sánchez, P. C., Fowler, D. M., Koulov, A., Kelly, J. W., *et al.* (2007) Semen-derived amyloid fibrils drastically enhance HIV infection. *Cell* **131,** 1059–1071
7. Tang, Q., Roan, N. R., and Yamamura, Y. (2013) Seminal plasma and semen amyloids enhance cytomegalovirus infection in cell culture. *J. Virol.* **87,** 12583–12591
8. Arnold, F., Schnell, J., Zirafi, O., Stürzel, C., Meier, C., Weil, T., Ständker, L., Forssmann, W. G., Roan, N. R., Greene, W. C., Kirchhoff, F., and Münch, J. (2012) Naturally occurring fragments from two distinct regions of the prostatic acid phosphatase form amyloidogenic enhancers of HIV infection. *J. Virol.* **86,** 1244–1249
9. Roan, N. R., Cavrois, M., and Greene, W. C. (2012) [Role of semen-derived amyloid fibrils as facilitators of HIV infection]. *Med. Sci.* **28,** 358–360
10. Roan, N. R., Müller, J. A., Liu, H., Chu, S., Arnold, F., Stürzel, C. M., Walther, P., Dong, M., Witkowska, H. E., Kirchhoff, F., Münch, J., and Greene, W. C. (2011) Peptides released by physiological cleavage of semen coagulum proteins form amyloids that enhance HIV infection. *Cell Host Microbe* **10,** 541–550
11. Roan, N. R., Münch, J., Arhel, N., Mothes, W., Neidleman, J., Kobayashi, A., Smith-McCune, K., Kirchhoff, F., and Greene, W. C. (2009) The cationic properties of SEVI underlie its ability to enhance human immunodeficiency virus infection. *J. Virol.* **83,** 73–80
12. Roan, N. R., Liu, H., Usmani, S. M., Neidleman, J., Müller, J. A., Avila-Herrera, A., Gawanbacht, A., Zirafi, O., Chu, S., Dong, M., Kumar, S. T., Smith, J. F., Pollard, K. S., Fändrich, M., Kirchhoff, F., Münch, J., Witkowska, H. E., and Greene, W. C. (2014) Liquefaction of semen generates and later degrades a conserved semenogelin peptide that enhances HIV infection. *J. Virol.* **88,** 7221–7234
13. Zirafi, O., Kim, K. A., Roan, N. R., Kluge, S. F., Müller, J. A., Jiang, S., Mayer, B., Greene, W. C., Kirchhoff, F., and Münch, J. (2014) Semen enhances HIV infectivity and impairs the antiviral efficacy of microbicides. *Sci. Transl. Med.* **6,** 262ra157
14. Grant, R. M., Hamer, D., Hope, T., Johnston, R., Lange, J., Lederman, M. M., Lieberman, J., Miller, C. J., Moore, J. P., Mosier, D. E., Richman, D. D., Schooley, R. T., Springer, M. S., Veazey, R. S., and Wainberg, M. A. (2008) Whither or wither microbicides? *Science* **321,** 532–534
15. Fichorova, R. N., Tucker, L. D., and Anderson, D. J. (2001) The molecular basis of nonoxynol-9-induced vaginal inflammation and its possible relevance to human immunodeficiency virus type 1 transmission. *J. Infect. Dis.* **184,** 418–428
16. Roan, N. R., Sowinski, S., Münch, J., Kirchhoff, F., and Greene, W. C. (2010) Aminoquinoline surfen inhibits the action of SEVI (semen-derived enhancer of viral infection). *J. Biol. Chem.* **285,** 1861–1869
17. Sievers, S. A., Karanicolas, J., Chang, H. W., Zhao, A., Jiang, L., Zirafi, O., Stevens, J. T., Münch, J., Baker, D., and Eisenberg, D. (2011) Structure-based design of non-natural amino-acid inhibitors of amyloid fibril formation. *Nature* **475,** 96–100
18. Hauber, I., Hohenberg, H., Holstermann, B., Hunstein, W., and Hauber, J. (2009) The main green tea polyphenol epigallocatechin-3-gallate counteracts semen-mediated enhancement of HIV infection. *Proc. Natl. Acad. Sci. U.S.A.* **106,** 9033–9038
19. Olsen, J. S., Brown, C., Capule, C. C., Rubinshtein, M., Doran, T. M., Srivastava, R. K., Feng, C., Nilsson, B. L., Yang, J., and Dewhurst, S. (2010) Amyloid-binding small molecules efficiently block SEVI (semen-derived enhancer of virus infection)- and semen-mediated enhancement of HIV-1 infection. *J. Biol. Chem.* **285,** 35488–35496
20. Capule, C. C., Brown, C., Olsen, J. S., Dewhurst, S., and Yang, J. (2012) Oligovalent amyloid-binding agents reduce SEVI-mediated enhancement of HIV-1 infection. *J. Am. Chem. Soc.* **134,** 905–908
21. Di Giovanni, S., Eleuteri, S., Paleologou, K. E., Yin, G., Zweckstetter, M., Carrupt, P. A., and Lashuel, H. A. (2010) Entacapone and tolcapone, two catechol *O*-methyltransferase inhibitors, block fibril formation of α-synuclein and β-amyloid and protect against amyloid-induced toxicity. *J. Biol. Chem.* **285,** 14941–14954
22. Ardah, M. T., Paleologou, K. E., Lv, G., Abul Khair, S. B., Kazim, A. S., Minhas, S. T., Al-Tel, T. H., Al-Hayani, A. A., Haque, M. E., Eliezer, D., and El-Agnaf, O. M. A. (2014) Structure activity relationship of phenolic acid inhibitors of α-synuclein fibril formation and toxicity. *Front. Aging Neurosci.* **6,** 197
23. Jayamani, J., and Shanmugam, G. (2014) Gallic acid, one of the components in many plant tissues, is a potential inhibitor for insulin amyloid fibril formation. *Eur. J. Med. Chem.* **85,** 352–358
24. Liu, Y., Pukala, T. L., Musgrave, I. F., Williams, D. M., Dehle, F. C., and Carver, J. A. (2013) Gallic acid is the major component of grape seed extract that inhibits amyloid fibril formation. *Bioorg. Med. Chem. Lett.* **23,** 6336–6340
25. Liu, Y., Carver, J. A., Calabrese, A. N., and Pukala, T. L. (2014) Gallic acid interacts with α-synuclein to prevent the structural collapse necessary for its aggregation. *Biochim. Biophys. Acta* **1844,** 1481–1485
26. Popovych, N., Brender, J. R., Soong, R., Vivekanandan, S., Hartman, K.,

Basrur, V., Macdonald, P. M., and Ramamoorthy, A. (2012) Site specific interaction of the polyphenol EGCG with the SEVI amyloid precursor peptide PAP(248–286). *J. Phys. Chem. B* **116,** 3650–3658

27. Castellano, L. M., Hammond, R. M., Holmes, V. M., Weissman, D., and Shorter, J. (2015) Epigallocatechin-3-gallate rapidly remodels PAP85–120, SEM1(45–107), and SEM2(49–107) seminal amyloid fibrils. *Biol. Open* **4,** 1206–1212

28. French, K. C., and Makhatadze, G. I. (2012) Core sequence of PAPf39 amyloid fibrils and mechanism of pH-dependent fibril formation: the role of monomer conformation. *Biochemistry* **51,** 10127–10136

29. Ye, Z., French, K. C., Popova, L. A., Lednev, I. K., Lopez, M. M., and Makhatadze, G. I. (2009) Mechanism of fibril formation by a 39-residue peptide (PAPf39) from human prostatic acidic phosphatase. *Biochemistry* **48,** 11582–11591

30. French, K. C., Roan, N. R., and Makhatadze, G. I. (2014) Structural characterization of semen coagulum-derived SEM1(86–107) amyloid fibrils that enhance HIV-1 infection. *Biochemistry* **53,** 3267–3277

31. Chen, J. C., Johnson, B. A., Erikson, D. W., Piltonen, T. T., Barragan, F., Chu, S., Kohgadai, N., Irwin, J. C., Greene, W. C., Giudice, L. C., and Roan, N. R. (2014) Seminal plasma induces global transcriptomic changes associated with cell migration, proliferation and viability in endometrial epithelial cells and stromal fibroblasts. *Hum. Reprod.* **29,** 1255–1270

32. Kim, S. H., Jun, C. D., Suk, K., Choi, B. J., Lim, H., Park, S., Lee, S. H., Shin, H. Y., Kim, D. K., and Shin, T. Y. (2006) Gallic acid inhibits histamine release and pro-inflammatory cytokine production in mast cells. *Toxicol. Sci.* **91,** 123–131

33. Yoon, C. H., Chung, S. J., Lee, S. W., Park, Y. B., Lee, S. K., and Park, M. C. (2013) Gallic acid, a natural polyphenolic acid, induces apoptosis and inhibits proinflammatory gene expressions in rheumatoid arthritis fibroblast-like synoviocytes. *Joint Bone Spine* **80,** 274–279

34. Robbins, K. J., Liu, G., Selmani, V., and Lazo, N. D. (2012) Conformational analysis of thioflavin T bound to the surface of amyloid fibrils. *Langmuir* **28,** 16490–16495

35. Sulatskaya, A. I., Kuznetsova, I. M., and Turoverov, K. K. (2012) Interaction of thioflavin T with amyloid fibrils: fluorescence quantum yield of bound dye. *J. Phys. Chem. B* **116,** 2538–2544

36. Shanmuganathan, A., Bishop, A. C., French, K. C., McCallum, S. A., and Makhatadze, G. I. (2013) Bacterial expression and purification of the amyloidogenic peptide PAPf39 for multidimensional NMR spectroscopy. *Protein Expr. Purif.* **88,** 196–200

37. Hudson, S. A., Ecroyd, H., Kee, T. W., and Carver, J. A. (2009) The thioflavin T fluorescence assay for amyloid fibril detection can be biased by the presence of exogenous compounds. *FEBS J.* **276,** 5960–5972

38. McCrate, O. A., Zhou, X., and Cegelski, L. (2013) Curcumin as an amyloid-indicator dye in *E. coli. Chem. Commun.* **49,** 4193–4195

39. Picken, M. M. (2010) Amyloidosis: where are we now and where are we heading? *Arch. Pathol. Lab. Med.* **134,** 545–551

40. Krainer, G., and Keller, S. (2015) Single-experiment displacement assay for quantifying high-affinity binding by isothermal titration calorimetry. *Methods* **76,** 116–123

41. Doane, T. L., Chuang, C. H., Hill, R. J., and Burda, C. (2012) Nanoparticle zeta-potentials. *Acc. Chem. Res.* **45,** 317–326

42. Kroes, B. H., van den Berg, A. J. J., Quarles van Ufford, H. C., van Dijk, H., and Labadie, R. P. (1992) Antiinflammatory activity of gallic acid. *Planta Med.* **58,** 499–504

43. Rollenhagen, C., and Asin, S. N. (2011) Enhanced HIV-1 replication in *ex vivo* ectocervical tissues from post-menopausal women correlates with increased inflammatory responses. *Mucosal Immunol.* **4,** 671–681

44. Herbein, G., Gras, G., Khan, K. A., and Abbas, W. (2010) Macrophage signaling in HIV-1 infection. *Retrovirology* **7,** 34

45. West, M. J., Lowe, A. D., and Karn, J. (2001) Activation of human immunodeficiency virus transcription in T cells revisited: NF-κB p65 stimulates transcriptional elongation. *J. Virol.* **75,** 8524–8537

46. Perkins, N. D., Edwards, N. L., Duckett, C. S., Agranoff, A. B., Schmid, R. M., and Nabel, G. J. (1993) A cooperative interaction between NF-κB and Sp1 is required for HIV-1 enhancer activation. *EMBO J.* **12,** 3551–3558

47. Sharkey, D. J., Tremellen, K. P., Jasper, M. J., Gemzell-Danielsson, K., and Robertson, S. A. (2012) Seminal fluid induces leukocyte recruitment and cytokine and chemokine mRNA expression in the human cervix after coitus. *J. Immunol.* **188,** 2445–2454

48. Sharkey, D. J., Macpherson, A. M., Tremellen, K. P., and Robertson, S. A. (2007) Seminal plasma differentially regulates inflammatory cytokine gene expression in human cervical and vaginal epithelial cells. *Mol. Hum. Reprod.* **13,** 491–501